

# Benchmarks for subduction zone models

## Updated December 2005

### Introduction

In early October 2002 a group of researchers met at the University of Michigan at Ann Arbor, MI to discuss the modeling of the thermal structure and dynamics of subduction zones ([www.geo.lsa.umich.edu/~keken/subduction02.html](http://www.geo.lsa.umich.edu/~keken/subduction02.html)). At the workshop it became clear that the community could greatly benefit from a set of benchmarks that allow for code testing and comparisons. We can identify two fundamental approaches for subduction zone modeling: a) fully dynamic, where the deformation of the slab is computed using descriptions of rheology and buoyancy; and b) wedge dynamical models, where the geometry and velocity of the slab is imposed kinematically, with a dynamic solution only for the wedge. This draft paper formulates a set of benchmarks of increasing complexity focusing on the second category. The first category requires a fundamentally more difficult approach. For a discussion of a number of potential dynamic benchmarks see [www.geobench.org](http://www.geobench.org). We hope that this set of benchmarks will evolve to a standard in subduction modeling, similar to the role of the mantle convection benchmarks formulated in Blankenbach et al., 1989; Busse et al., 1993; and Van Keken et al., 1997.

### Description of governing equations and parameters

Conservation of mass for incompressible fluid:

$$\nabla \cdot \mathbf{v} = 0 \quad (1)$$

Heat transport equation for an incompressible medium:

$$\rho c_p (\mathbf{v} \cdot \nabla) T = \nabla \cdot (k \nabla T) + Q + Q_{sh} \quad (2)$$

Conservation of momentum for viscous flow:

$$\nabla \cdot \boldsymbol{\tau} - \nabla P = \mathbf{0} \quad (3)$$

with deviatoric stress tensor  $\boldsymbol{\tau}$ :

$$\boldsymbol{\tau} = 2\eta \dot{\boldsymbol{\epsilon}} \quad (4)$$

and components of the strain rate tensor  $\dot{\boldsymbol{\epsilon}}$ :

$$\dot{\epsilon}_{ij} = \frac{1}{2} \left[ \frac{\partial u_i}{\partial x_j} + \frac{\partial u_j}{\partial x_i} \right] \quad (5)$$

The effective shear viscosity  $\eta$  follows from (4):

$$\eta = \frac{\tau}{2\dot{\epsilon}} \quad (6)$$

where the second invariants of the strain-rate and stress tensors are defined by  $\dot{\epsilon} = \left[ \frac{1}{2} \sum_{ij} \dot{\epsilon}_{ij} \dot{\epsilon}_{ij} \right]^{\frac{1}{2}}$  and

$$\tau = \left[ \frac{1}{2} \sum_{ij} \tau_{ij} \tau_{ij} \right]^{\frac{1}{2}}.$$

A general equation for the viscosity of olivine deformation by diffusion creep is

$$\eta_{diff}(T) = A_{diff} e^{(E_{diff} + pV_{diff})/RT} \quad (7)$$

and for deformation by dislocation creep

$$\eta_{disl}(T, \dot{\epsilon}) = A_{disl} e^{(E_{disl} + pV_{disl})/nRT} \dot{\epsilon}^{(1-n)/n} \quad (8)$$

See, for example, Karato and Wu (1993).

### Definition of symbols

Quantity	Symbol	Reference value and/or SI units
Velocity	$\mathbf{v}$	m/s
Dynamic viscosity	$\eta$	$\eta_0 = 10^{21}$ Pa · s
Stress tensor	$\tau$	Pa
Strain rate tensor	$\dot{\epsilon}$	1/s
Dynamic pressure	$P$	Pa
Dynamic pressure gradient	$\nabla P$	Pa/m
Density	$\rho$	$\rho_0 = 3300$ kg/m <sup>3</sup>
Temperature	$T$	$T_0 = 1573$ K = 1300 °C
Thermal conductivity	$k$	$k = 3$ W/mK
Heat capacity	$c_p$	1250 J/kgK
Radiogenic heating	$Q$	W/m <sup>3</sup>
Shear heating	$Q_{sh}$	W/m <sup>3</sup>
Thermal diffusivity	$\kappa = k/\rho c_p$	$0.7272 \times 10^{-6}$ m <sup>2</sup> /s
Activation energy for diffusion creep	$E_{diff}$	335 kJ/mol
Activation energy for dislocation creep	$E_{disl}$	540 kJ/mol
Powerlaw exponent for dislocation creep	$n$	3.5
Pre-exponential constant for diffusion and dislocation creep	$A_{diff}, A_{disl}$	Pa · s <sup>1/n</sup>
Hydrostatic pressure	$p$	Pa
Activation volume for diffusion and dislocation creep	$V_{diff}, V_{disl}$	0 m <sup>3</sup> /mol
Gas constant	$R$	8.3145 J/molK

All models are 2D Cartesian (assuming no variation in the third dimension). For simplicity we will not make a distinction between potential and 'real' temperature.

### Model description

Computational domain: box of 660x600 km (see Figure 1). Straight slab at 45 degree angle. The top of slab starts in the upper left hand corner at ( $x = 0$  km,  $z = 0$  km). The mantle below the slab moves with the same velocity  $\mathbf{V}_0$ . The speed of the slab is  $|\mathbf{V}_0| = 5$  cm/yr. The overriding plate above the wedge is assumed rigid and extends to a depth of 50 km. Reference values for  $k$ ,  $\rho$ , and  $c_p$ . Note that this yields a value for  $\kappa = 0.7272 \cdot 10^{-6}$  m<sup>2</sup>/s. No radiogenic or shear heating. Age of the incoming lithosphere at  $x=0$  is 50 Myr, projected vertically onto the side wall boundary.

In benchmark 1 we formulate three different cases that differ in the treatment of the velocity in an isoviscous wedge of viscosity  $\eta_0$ . Case 1a uses the Batchelor analytical solution for the corner-flow and is therefore strictly an advection-diffusion problem for heat. Case 1b requires solution of the Stokes equation in the isoviscous wedge but with the Batchelor solution imposed on the inflow and outflow boundaries. This case tests the ability of the methods to accurately reproduce

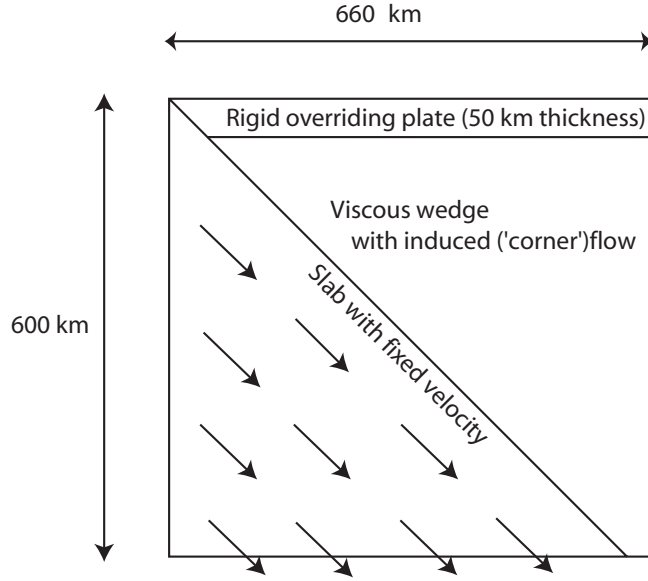


Figure 1 Geometry of the subduction zone benchmark

the Batchelor solution. In case 1c the in- and outflow boundary conditions are stress-free rather than imposed velocity.

In benchmark 2 we formulate two cases that differ in the rheological description of the wedge. Case 2a uses a temperature-dependent viscosity following the diffusion creep of olivine with constant grain-size. Case 2b uses a temperature- and strain-rate-dependent viscosity based on the dislocation creep in olivine.

The benchmark models explicitly treat the 'seismogenic zone' from (0,0) to (50,50) as a fault with discontinuous velocity. On the slab side the velocity is always  $\mathbf{V} = \mathbf{V}_0$ , on the overriding plate side the velocity is always  $\mathbf{V} = \mathbf{0}$ . In case 1a the velocity along the slab-wedge interface is  $\mathbf{V} = \mathbf{V}_0$  and the velocity internal to the wedge is defined by the Batchelor analytical solution. The velocity description changes at (50,50). From the seismogenic zone perspective this point has velocity  $\mathbf{V} = \mathbf{V}_0$  along the slab,  $\mathbf{V} = \mathbf{0}$  along the overriding plate but below this point the velocity is continuous across the slab wedge interface. We recommend treating this point as part of the seismogenic zone with discontinuous velocity.

When the Stokes solution is solved the boundary conditions at the top of the slab require special attention. The Batchelor cornerflow description has discontinuous velocity at the cornerpoint (50,50) which causes a singularity in pressure. While this singularity is integrable, it is known to influence the accuracy of the discrete solution of most methods even when very high resolution is used. We modify the boundary condition for the wedge flow in such a way that velocity is continuous, by letting the velocity increase linearly from  $\mathbf{V} = \mathbf{0}$  at (50,50) to  $\mathbf{V} = \mathbf{V}_0$  a short distance downstream from the cornerpoint. Formally, we change the boundary condition along the slab-wedge interface from

$$\mathbf{v}(\mathbf{x}_{slab-wedge}) = \mathbf{V}_0 \tag{9a}$$

to

$$\begin{aligned} \mathbf{v}(\mathbf{x}_{slab-wedge}) &= \frac{\mathbf{x} - \mathbf{x}_{corner}}{\mathbf{x}_{full-coupling} - \mathbf{x}_{corner}} \mathbf{V}_0 & \mathbf{x}_{corner} \leq \mathbf{x} \leq \mathbf{x}_{full-coupling} \\ \mathbf{v}(\mathbf{x}_{slab-wedge}) &= \mathbf{V}_0 & \mathbf{x} \geq \mathbf{x}_{full-coupling} \end{aligned} \quad (9b)$$

where  $\mathbf{x}_{slab-wedge}$  is the position of the slab-wedge interface,  $\mathbf{x}_{corner}$  is the cornerpoint (50,50), and  $\mathbf{x}_{full-coupling}$  is the position down-slab where full coupling is achieved. This should be a short distance  $D$  from the cornerpoint so that,

$$\mathbf{x}_{full-coupling} = \mathbf{x}_{corner} + \sqrt{D} \mathbf{I} \quad (9c)$$

Tests show that with a resolution on the order of a km and a transition length on the order of a few km (or better) provides an adequate match to the Batchelor solution. The velocity ramp is on the wedge side only and this short segment should be treated as an extension of the fault from (0,0) to (50,50). This transition can be thought of as a healing fault, where the velocity description changes from that of a discontinuous fault (with  $\mathbf{V} = \mathbf{0}$  at the side of the wedge and overriding plate;  $\mathbf{V} = \mathbf{V}_0$  at the slab side) to a fully coupled zone (with  $\mathbf{V} = \mathbf{V}_0$  on both sides of the slab-wedge interface).

The cases with variable rheology have viscosity in the wedge based on the general form (7)+(8) with a (maximum) viscosity cut-off. Since the flow in the wedge is driven purely kinematically, the range of dynamic viscosity influences the solution. This effect is particularly strong near the return flow in the corner point. A large dynamic range in viscosity leads in this case to deformation and unrealistic high stresses in the high viscosity regions. In order to avoid this physically unrealistic situation the effective viscosity follows from a truncation of the olivine creep laws following

$$\eta_{diff, effective} = \left( \frac{1}{\eta_{diff}} + \frac{1}{\eta_{max}} \right)^{-1} \quad (11)$$

$$\eta_{disl, effective} = \left( \frac{1}{\eta_{disl}} + \frac{1}{\eta_{max}} \right)^{-1} \quad (12)$$

where  $\eta_{diff}$  follows from (7),  $\eta_{disl}$  from (8), and  $\eta_{max}$  is the maximum viscosity.

## Description of the benchmark cases

### 1a) Temperature field with isoviscous wedge using the analytical Batchelor solution.

Use the analytical expression for cornerflow (e.g., Batchelor, 1967) to describe (u,v). This model requires only the solution of the temperature equation with the following boundary conditions:  $T_s = 273$  K at the surface.  $T_m = 1573$  K at the inflow portion of the wedge (below the overriding plate). This results in a linear temperature gradient in the overriding plate at the left hand boundary. The temperature at the slab inflow boundary is described by the standard error function consistent with the 50 Myr age of the lithosphere

$$T(z) = T_s + (T_m - T_s) \operatorname{erf} \left( \frac{z}{2\sqrt{\kappa T_{50}}} \right) \quad (10)$$

where  $T_{50}$  is the age of the lithosphere in seconds. At the slab and wedge outflow boundaries:  $\nabla T \cdot \mathbf{n} = 0$ . Specify  $P = 0$  at the inflow boundary at the interface between overriding plate and wedge ( $x = 660$  km,  $z = 50$  km).

*1b) Dynamically computed wedge flow with constant viscosity - 1.*

As in a), but now with a dynamical solution for the velocity in the wedge only. The flow is kinematically driven by the slab (i.e., no buoyancy due to thermal expansion). In order to compare results with a) we will describe the same boundary conditions for velocity: velocity is 0 at the top of the wedge. The velocity is equal to the slab velocity at the slab-wedge interface. The velocity of the inflow and outflow boundary are imposed by the Batchelor solution. See for example the results shown in Appendix A of Van Keken et al. (2003).

*1c) Dynamically computed wedge flow with constant viscosity - 2.*

As in b), but now with natural boundary conditions for stress at the inflow and outflow boundary. Both the normal and the tangential component of the total stress  $\tau - P\mathbf{I}$ , where  $\mathbf{I}$  is the identity tensor should be set to zero.

*2a) Dynamical wedge with diffusion creep*

Use the formulation (11) for the effective viscosity for diffusion creep in olivine with  $E_{diff} = 335$  kJ/mol,  $V_{diff} = 0$ , and pre-exponential factor  $A_{diff} = 1.32043 \times 10^9$  Pa · s, and  $\eta_{max} = 10^{26}$  Pa · s. This prefactor follows from the arbitrary assumption that  $\eta = \eta_0$  at 1473 K.

*2b) Dynamical wedge with dislocation creep*

Use the formulation (12) for the effective viscosity for dislocation creep in olivine with  $E_{disl} = 540$  kJ/mol,  $V_{disl} = 0$ ,  $n = 3.5$ , and pre-exponential factor  $A_{disl} = 28968.6$  Pa · s<sup>1/n</sup> (corresponding to the dislocation creep parameters of Karato and Wu, 1993), and  $\eta_{max} = 10^{26}$  Pa · s.

## **Requested output**

For each of these models provide

### **Required:**

2D arrays of  $T$ ,  $P$ ,  $dT/dx$ ,  $dT/dz$ ,  $dP/dx$  and  $dP/dz$ . Provide these quantities at  $x_i, z_j$ , where  $x_i = (i-1)\Delta x$  and  $z_j = (j-1)\Delta z$  with  $\Delta x = \Delta z = 6$  km. This allows us to difference various solutions as function of type of code, assumptions about boundary conditions and resolution of the computational grid. Also provide heat flow in this output grid points at the surface ( $x_i, 0$ ).

*Format of the output files.* Please provide these quantities in **dimensional** units ( $T$  in °C,  $P$  in MPa, heat flow in W/m<sup>2</sup>, and the pressure and temperature derivatives in MPa/km and °C/m). The 2D arrays should be in ASCII (text) files with 101 rows, each containing 111 numbers. The top row corresponds to the surface of the model.

### **Optional:**

Integrated quantities, e.g., rms-velocity, average temperature, average pressure, and average dissipation in the wedge.

## Optional test for convection dominated flows

### Model description

#### a) Transport of smooth function

As in 1a (isoviscous wedge using analytical Batchelor solution) but with low diffusivity and variable temperature at inflow boundary, e.g.,

$$T(0, z) = \cos(n\pi(z - z_0)/\lambda)$$

where  $z_0$  is the thickness of the overriding plate (50 km) and  $\lambda$  is the distance between the base of the overriding plate and the transition between in- and outflow of the Batchelor solution. Use  $n = 1, n = 3, n = 5 \dots$ .

#### b) Transport of discontinuous function

As in 3a), but now with a discontinuous function of the form

$$T(0, z) = T_0 \quad \text{if } \cos(n\pi(z - z_0)/\lambda) \leq 0$$

$$T(0, z) = T_0 + \Delta T \quad \text{if } \cos(n\pi(z - z_0)/\lambda) > 0$$

### Requested output:

Show the temperature at the outflow boundary of the wedge.

### References

- Batchelor, G.K., An introduction to fluid dynamics, 615 pp., Cambridge University Press, New York, 1967.
- Blankenbach, B., F. Busse, U. Christensen, L. Cserepes, D. Gunkel, U. Hansen, H. Harder, G. Jarvis, M. Koch, G. Marquart, D. Moore, P. Olson, H. Schmeling, T. Schnaubelt, A benchmark comparison for mantle convection codes, *Geophys. J. Int.*, 98, 23-38, 1989.
- Busse, F.A., Christensen, U., Clever, R., Cserepes, L., Giannandrea, E., Guillou, L., Nataf, H.-C., Ogawa, M., Parmentier, M., Sotin, C., and Travis, B, Convection at infinite Prandtl number in Cartesian geometry - a benchmark comparison. *Geophys. Astrophys. Fluid Dyn.*, 75, 35-59, 1993.
- Karato, S., and P. Wu, Rheology of the upper mantle: a synthesis, *Science*, 260, 771-778, 1993.
- Van Keken, P.E., King, S.D., Schmeling, H., Christensen, U.R., Neumeister, D., Doin, M.P., A comparison of methods for the modeling of thermochemical convection, *J. Geophys. Res.*, 102, 22,477-22,495, 1997.
- Van Keken, P.E., B. Kiefer, and S. Peacock, High resolution models of subduction zones: implications for mineral dehydration reactions and the transport of water into the deep mantle, *Geochemistry, Geophysics, and Geosystems*, 3, 2002. doi: 10.1029/2001GC000256.